



Localization and Ordering of Lipids Around Aquaporin-0: Protein and Lipid Mobility Effects

Rodolfo Briones¹, Camilo Aponte-Santamaría² and Bert L. de Groot^{1*}

¹ Computational Biomolecular Dynamics Group, Max Planck Institute for Biophysical Chemistry, Göttingen, Germany,

² Molecular Biomechanics Group, Heidelberg Institute for Theoretical Studies and Interdisciplinary Center for Scientific Computing, Heidelberg, Germany

OPEN ACCESS

Edited by:

Rainer A. Böckmann,
University of Erlangen-Nuremberg,
Germany

Reviewed by:

Jesus Perez-Gil,
Complutense University of Madrid,
Spain

Rodrigo F. M. De Almeida,
Universidade de Lisboa, Portugal

*Correspondence:

Bert L. de Groot
bgroot@gwdg.de

Specialty section:

This article was submitted to
Membrane Physiology and Membrane
Biophysics,
a section of the journal
Frontiers in Physiology

Received: 28 November 2016

Accepted: 15 February 2017

Published: 02 March 2017

Citation:

Briones R, Aponte-Santamaría C and
de Groot BL (2017) Localization and
Ordering of Lipids Around
Aquaporin-0: Protein and Lipid
Mobility Effects. *Front. Physiol.* 8:124.
doi: 10.3389/fphys.2017.00124

Hydrophobic matching, lipid sorting, and protein oligomerization are key principles by which lipids and proteins organize in biological membranes. The Aquaporin-0 channel (AQP0), solved by electron crystallography (EC) at cryogenic temperatures, is one of the few protein-lipid complexes of which the structure is available in atomic detail. EC and room-temperature molecular dynamics (MD) of dimyristoylglycerophosphocholine (DMPC) annular lipids around AQP0 show similarities, however, crystal-packing and temperature might affect the protein surface or the lipids distribution. To understand the role of temperature, lipid phase, and protein mobility in the localization and ordering of AQP0-lipids, we used MD simulations of an AQP0-DMPC bilayer system. Simulations were performed at physiological and at DMPC gel-phase temperatures. To decouple the protein and lipid mobility effects, we induced gel-phase in the lipids or restrained the protein. We monitored the lipid ordering effects around the protein. Reducing the system temperature or inducing lipid gel-phase had a marginal effect on the annular lipid localization. However, restraining the protein mobility increased the annular lipid localization around the whole AQP0 surface, resembling EC. The distribution of the inter-phosphate and hydrophobic thicknesses showed that stretching of the DMPC annular layer around AQP0 surface is the mechanism that compensates the hydrophobic mismatch in this system. The distribution of the local area-per-lipid and the acyl-chain order parameters showed particular fluid- and gel-like areas that involved several lipid layers. These areas were in contact with the surfaces of higher and lower protein mobility, respectively. We conclude that the AQP0 surfaces induce specific fluid- and gel-phase prone areas. The presence of these areas might guide the AQP0 lipid sorting interactions with other membrane components, and is compatible with the squared array oligomerization of AQP0 tetramers separated by a layer of annular lipids.

Keywords: lipid-protein interactions, annular lipids, lens aquaporin-0, molecular dynamics simulations, hydrophobic matching, lipid thinning, membrane protein lipid sorting

1. INTRODUCTION

The interplay between lipids and membrane proteins plays a fundamental role in biological membranes (Marsh, 2008; Lee, 2011). Our current understanding of the lipid-protein dynamics indicates that both, proteins, and lipids might undergo correlated structural changes that influence the assembly, organization, and ultimately the function of biological membranes (Killian, 1998; de Planque and Killian, 2003; Lee, 2003). These changes appear to be largely triggered by

the minimization of the hydrophobic areas exposed to the aqueous solutions of the membrane proteins—or peptides—and the lipids around them, concept known as hydrophobic matching (Killian, 1998). Experimental and computational studies have shown in detail how peptides in membranes locally affect each other due to hydrophobic mismatch. A peptide might change its conformation, orientation, or oligomerization state in the membrane. In addition, the lipids might locally adapt by thickening or thinning around an embedded peptide. Recruiting of specific lipids around proteins (lipid sorting), or selective partitioning of proteins in certain lipids (rafts) are other possible mechanisms in real, complex, and multicomponent biological membranes (Piknová et al., 1993; Dumas et al., 1997; Killian, 1998; de Planque and Killian, 2003). However, the molecular determinants between integral membrane proteins and their surrounding lipids remain partially unresolved. In this work, by using a single component model membrane, we studied the effect of temperature, lipid gel-phase, and reduced protein mobility on the lipid distribution around the integral membrane protein aquaporin-0 (AQP0).

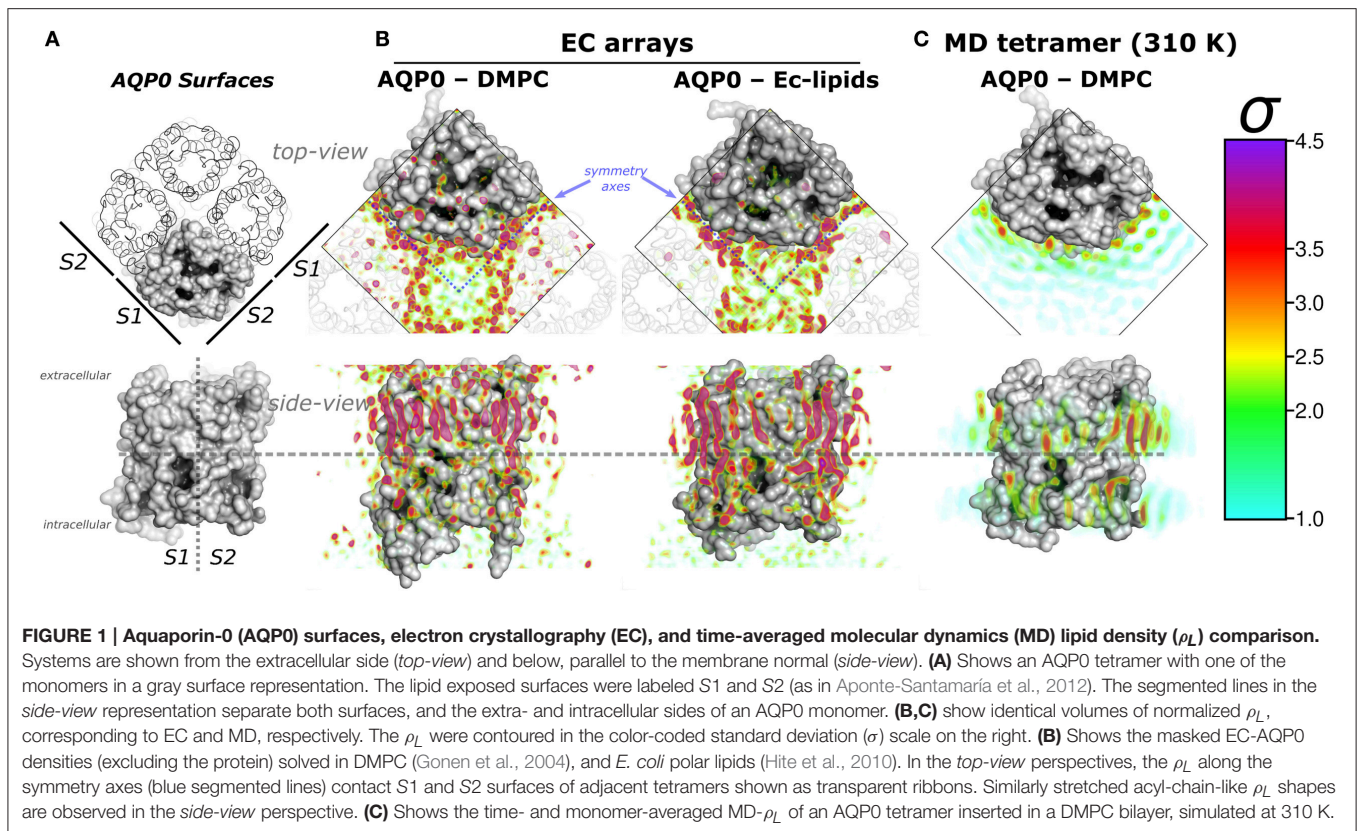
Several studies have shown how membranes are affected by the presence of peptides or proteins under different hydrophobic matching conditions. Simulations of the gramicidin A peptide in different membranes showed that its presence introduces structural and dynamic changes in and beyond the annular lipid layer (Kim et al., 2012). The KALP, WALP, and related α -helical peptides have illustrated that peptide tilting, association, lipid thinning or thickening, and specific lipid–amino acid interactions are involved in the peptide–lipid response under different hydrophobic mismatch conditions (de Planque and Killian, 2003; Kandasamy and Larson, 2006; Kim and Im, 2010; Monticelli et al., 2010). Bigger integral membrane proteins like the potassium channel KcsA were found to locally reduce the diffusion of its annular lipids (Niemelä et al., 2010). Experimental studies on bacteriorhodopsin (bR) have shown that its presence is capable of recruiting lipids (Dumas et al., 1997), and inducing temperature shifts in the phase transition of glycerophospholipids (Piknová et al., 1993). Thinning of membranes around an aquaporin-0 (AQP0) tetramer have also been reported (Stansfeld et al., 2013). In addition, several copies of membrane proteins (including AQP0) inserted in model membranes at physiological concentrations, are able to modify the membrane stiffness (Fowler et al., 2016). Mass spectrometry experiments in combination with MD simulations revealed a broad range of lipid binding affinities for membrane proteins, which critically influence their structural stability, oligomerization state, and function (Laganowsky et al., 2014; Landreh et al., 2016; Gupta et al., 2017). State of the art simulations have shown that is possible to study lipid sorting of small proteins in binary lipid mixtures (Yin and Kindt, 2012). Nevertheless, protein simulations in the presence of cholesterol considerably reduce the diffusion of the lipid components (O'Connor and Klauda, 2011), which in turn increases the simulation times necessary for equilibration and sampling, beyond the multi-microsecond scales (Baker and Abrams, 2014).

AQP0 is one of the few membrane protein that provides atomistic details of protein–lipid complexes. AQP0 monomers

arrange functionally as homotetramers, and are exclusively expressed in fiber lens cell membranes, where they allow water permeation and mediate intermembrane junctions (Chepelinsky, 2009). As shown by electron- (Costello et al., 1989), atomic force- (Colom et al., 2012) (AFM), and hybrid high-speed atomic force–optical microscopy (Colom et al., 2013), AQP0 is able to natively form self assembled 2D tetramer array domains. Electron crystallography (EC) (Gonen et al., 2004, 2005; Hite et al., 2010) of 2D crystal arrays of reconstituted AQP0–phospholipids have shown the molecular details of the AQP0 structure surrounded by a lipid shell (also called annular lipids) to a resolution below 2 Å. A similar single layer of the electron densities, refined as lipid molecules (ρ_L), formed a compact layer of annular lipids, sandwiched between AQP0 tetramers, was observed either with the single component membrane dimyristoylglycerophosphocholine (DMPC) or with the non native *E. coli* polar lipids (**Figures 1A,B**). These lipids are different to the native lipid composition of the ocular lens membranes that consist mainly of sphingomyelin, and a highly variable cholesterol content (Borchman and Yappert, 2010). Nevertheless, the lattice parameters of the *in vivo* AQP0 arrays (Colom et al., 2012, 2013) are identical to those of EC structures. Thus, AQP0 (in particular surrounded by DMPC lipids) constitutes an ideal system to study lipid–protein interactions. This information also indicates that AQP0 tetramer array formation is possible under different hydrophobic matching circumstances. Furthermore, it suggests that the lipid accommodation observed here for DMPC may also occur for other more physiologically relevant lipid species beyond *E. coli* polar lipids.

In the eye lens membranes most of the lipids are associated with proteins and the lipid composition varies considerably at different parts of the lens (Borchman and Yappert, 2010). These proteins include around 60% of AQP0 and 15% of connexins (Colom et al., 2012). Other important proteins are the plasma membrane Ca^{+2} –ATPase, and the Na,K–ATPase, which are necessary to keep the ion homeostasis and lens clarity (Borchman and Yappert, 2010). From atomic force microscopy on lens fiber cells (Colom et al., 2012), an interaction energy of $-2.7 k_B T$ between AQP0 tetramers was estimated. Using this energy value in 2D Monte Carlo simulations gave an estimated value of 1% of free AQP0 tetramers. The native membrane composition of human fiber lens includes variable cholesterol content and longer dihydrosphingomyelin lipids, which contain 60% of palmitoyl (C16:0) and 25% nervonoyl (C24:1 ω 9) acyl-chains (Borchman and Yappert, 2010). Although, the *in vivo* molecular details of the AQP0–lipids interfaces is not known, it most likely to vary at different parts of the eye lens membranes, therefore the 2D-arrays found in electron crystallography (Gonen et al., 2004; Hite et al., 2010) do represent physiologically relevant states captured by AFM (Colom et al., 2012, 2013).

Remarkably, EC- and MD- ρ_L of DMPC around AQP0 show similar localization (Aponte-Santamaría et al., 2012). These ρ_L s depict 7–9 annular lipids per monomer, that show higher intensity and more straightened densities at the extracellular leaflet (**Figures 1A,B**). ρ_L shapes and intensities are especially similar at the S2 surface, where a higher ρ_L is observed by MD

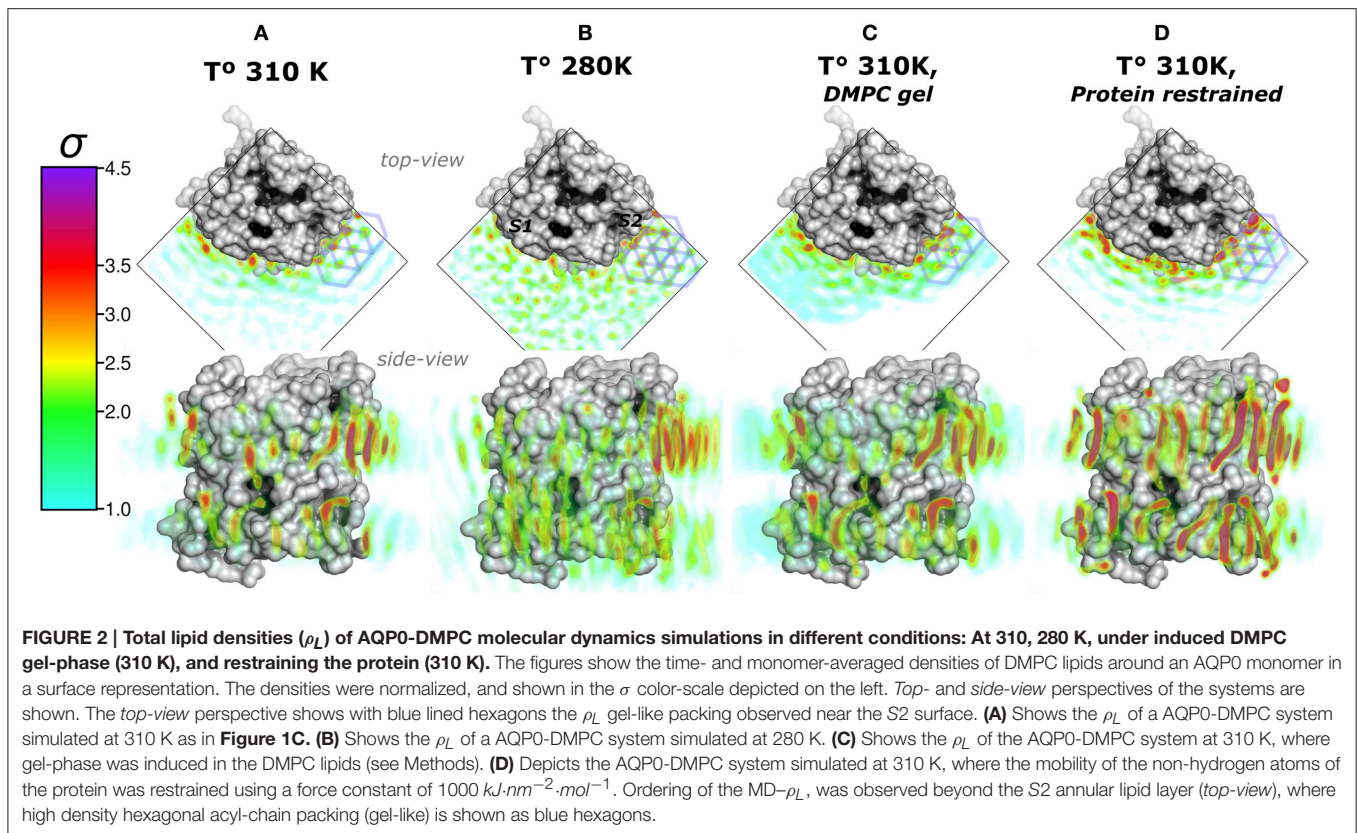


at room-temperature (Aponte-Santamaría et al., 2012), and also at physiological temperature (Figure 1C). The identified driving principles of the annular lipid localization around AQP0 were of protein origin, these principles were found to consist of a combination of favorable van der Waals interactions, protein-lipid surface complementarity, and protein mobility (Aponte-Santamaría et al., 2012). This evidence indicates that the protein guides the lipid distribution, and little influence on the protein is exerted by the lipids. Although, we cannot rule out the possibility that other lipids might exert structural protein changes, the two AQP0 structures, solved in different lipid environments (DMPC and *E. coli* lipids) (Gonen et al., 2004; Hite et al., 2010), were found to be highly similar (with a backbone RMSD below 1 Å). This suggests different lipid components to promote protein structural effects only to a minor extent in AQP0.

However, cryogenic temperatures and crystallographic packing might alter the protein-lipids mobility. Considering the fact that AQP0 forms similar 2D arrays in model as well as in native membranes, it is reasonable to think that the molecular determinants of the protein-lipids interactions might be also similar. In this work we want to understand how do (a) lipids shape the protein surface, and (b) protein (mobility) shape the lipid localization and ordering. For that purpose, we simulated a single AQP0 tetramer inserted in a DMPC bilayer at physiological (310 K), and at DMPC gel-phase temperature (280 K). To decouple the protein and lipid mobility effects, we induced gel-phase in the lipids, or restrained the protein.

2. METHODS

Molecular dynamic simulations were performed with GROMACS 5.0 (Abraham et al., 2015) software package on an AQP0-DMPC system, which consisted of 4 AQP0 monomers (PDB id: 3M9I; Hite et al., 2010), 392 DMPC (C14:0) lipid molecules, water, and 150 [mM] NaCl. Using the constant particle ($\sim 140,000$ atoms), isothermic, isobaric (1 bar) ensemble (NPT), Systems in different “mobility” conditions were pre-equilibrated. Namely: 1. $T = 310$ K (37 °C, physiological); unrestrained system, equilibration time: 100 ns. 2. $T = 280$ K (7 °C); DMPC at gel-phase (L_β) and not ice-water, equilibration time: 400 ns. 3. $T = 310$ K; induced DMPC-gel by changing the water model, equilibration time: 280 ns. The modified CHARMM water model (MacKerell et al., 1998) keeps the DMPC system in the fluid phase at 310 K (L_α). However, the original TIP3P water (Jorgensen et al., 1983), induces gel-phase, as it is known for C36 lipids (Pastor and MacKerell, 2011; Boonstra et al., 2016). 4. $T = 310$ K; a protein restrained system, with a reduced protein mobility was obtained by applying a force constant of $k = 1000$ kJ/(nm² mol) on the non-hydrogen atoms, equilibration time: 170 ns. Protein (Bjelkmar et al., 2010) and lipids used CHARMM forcefields (Klauda et al., 2010). An integration time step of 2 fs was used with Verlet algorithm (Swope, 1982). The PME algorithm was used for electrostatic interactions (Essmann et al., 1995). Potential-shift with the Verlet cutoff-scheme from 0.8 to 1.0 nm was used for short range



electrostatic and van der Waals interactions. The V-rescale (Bussi et al., 2007) and the Parrinello-Rahman (Nosé and Klein, 1983) algorithms were used for temperature and pressure coupling.

The lipid densities (MD- ρ_L) were estimated from 280 ns MD trajectories using a modified software tool, which allows to calculate the time-averaged density of molecule(s) around e.g., a protein (Aponte-Santamaría et al., 2012). The implemented grid based approach, considered the atomic scattering factors taken from Hirai et al. (2007). The trajectories were pre-processed to account for the four-fold symmetry of AQP0 structures. The local lipid ordering was estimated with g_{Lomepro} (Gapsys et al., 2013) in a 100×100 grid. The calculated lipid properties were: inter-phosphorous (P-P), and hydrophobic thicknesses, the later using the carbon-2 average position from both acyl-chains (Kim et al., 2012); the area-per-lipid (APL), and the carbon-deuterium order parameters (S_{CD}). The interaction energies and protein fluctuations (RMSF) were estimated with Gromacs tools. The rendering of molecular images was done with the software Pymol (Schrödinger, 2015).

3. RESULTS AND DISCUSSION

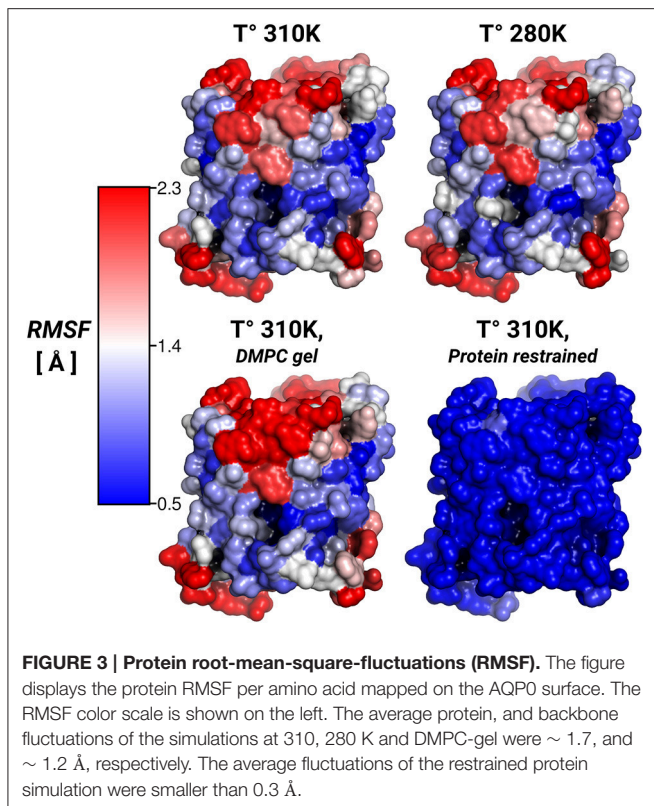
In the EC structures, the electron densities refined as lipid molecules (ρ_L) contact the two AQP0 symmetry related surfaces (termed S1 and S2) of adjacent tetramers. Representations of AQP0 surfaces and the EC ρ_L are shown in **Figures 1A,B**. At physiological temperature, the average MD- ρ_L of an AQP0

tetramer inserted in DMPC is shown in **Figure 1C**. By changing the AQP0-DMPC system mobility we want to understand how the temperature, induced lipid gel-phase, and restraining the protein contribute to the localization and ordering of unconstrained lipids around AQP0.

3.1. Lipids Localization

We first addressed the localization of the annular lipids by comparing the changes in the total ρ_L . In **Figure 2** the lipid densities of simulations at 310, 280 K, under induced DMPC gel-phase, and with the protein restrained were compared. The ρ_L at 280 K (**Figure 2B**) and the DMPC-gel at 310 K (**Figure 2C**) displayed similar higher annular ρ_L at the extracellular side, and ρ_L was more localized at S2 than S1, compared to those of the unrestrained system at 310 K (**Figure 2A**). A similar ρ_L distribution was observed at 300 K (Aponte-Santamaría et al., 2012). In contrast, the simulation with the protein restrained showed a considerable increase of the annular ρ_L throughout the AQP0 surface (**Figure 2D**). The extent of this density increase made the annular ρ_L similar to those in EC (**Figure 1B**).

In order to test whether the ρ_L asymmetry between surfaces S1 and S2 was influenced by sampling, we increased the simulated time used to calculate the MD- ρ_L in the unrestrained simulation at 310 K by a factor of ten, from 280 ns to $2.8 \mu\text{s}$ (Figure S1). We observed that using $2.8 \mu\text{s}$, the qualitative ρ_L localization was similar as for 280 ns. Nevertheless, by using $2.8 \mu\text{s}$ the ρ_L intensities decreased considerably mostly on S1. This result

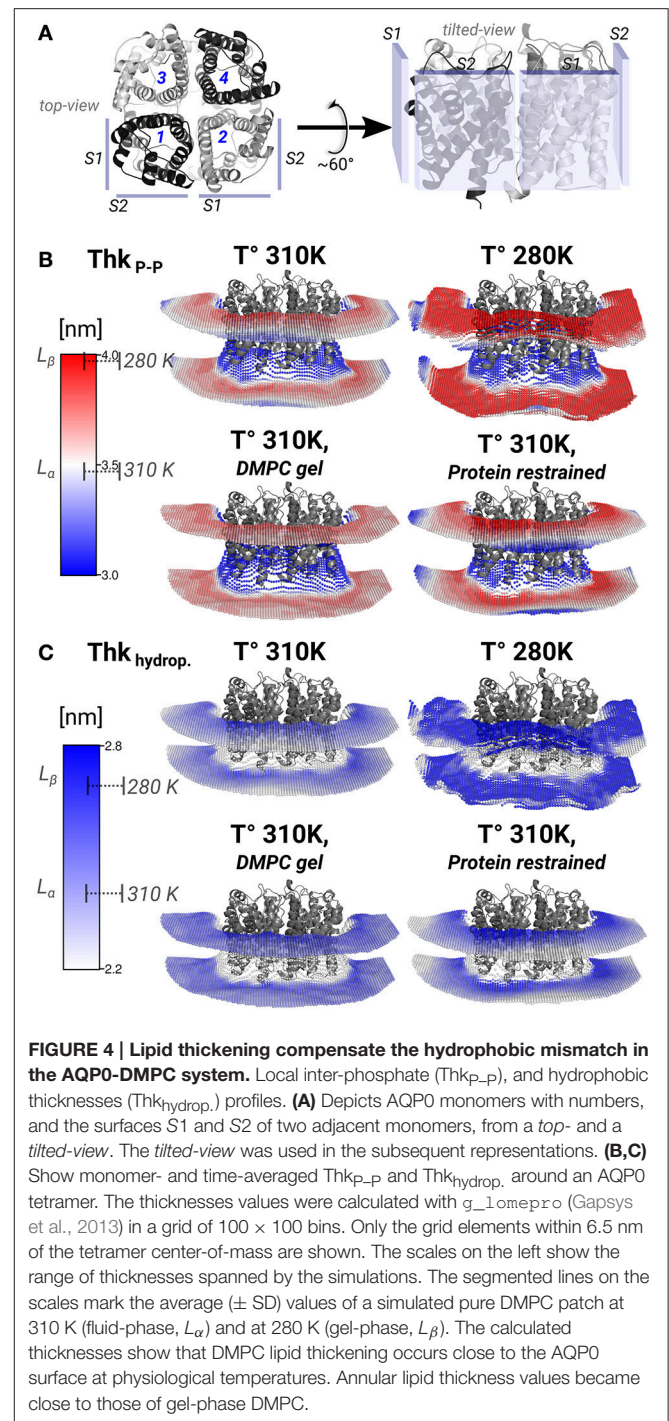


showed that annular lipids have a localization preference on the surface S2, especially at the extracellular side.

High ρ_L was also observed beyond the annular lipid layer in all conditions and mostly around the extracellular part of S2 (*top-view* perspectives in **Figure 2**). These ρ_L s displayed the characteristic hexagonal packing of DMPC acyl-chains in the gel-phase (L_β) (Smith et al., 1990; Akabori and Nagle, 2015). Gel-like lipids were expected in the 280 K simulation and in the induced DMPC-gel simulations. Nevertheless, these gel-like ρ_L s were also observed in the unrestrained and in the protein restrained simulations at 310 K. Such hexagonal pattern of ρ_L s included 4 acyl-chains of the highly localized annular lipids and extended clearly to several lipid layers as it is observed in the protein restrained and 280 K simulations. This evidence suggests that S2 induces local gel-phase changes in the surrounding membrane.

3.2. Lipids Interactions and Protein Fluctuations

Higher annular lipid densities on the AQP0 surfaces are an indication of favorable interactions between the lipids and the protein surface. The lipid localization may be due to global interactions of the different components of the AQP0-DMPC-water system, or to specific interactions with amino acids on the AQP0 surface. These interactions might change with the DMPC lipids in the gel-phase. In addition, we wondered if the gel-phase transition of the lipids may lead to reduced protein mobility.



To understand the protein-lipid interactions, we estimated the global interaction energies of DMPC lipids with other DMPC molecules (self), with the protein, and with water. We also decomposed the lipid-amino acid interaction energies in vdW and electrostatic components, and mapped these values on the AQP0 surface. The results of both procedures are shown in Figures S2A–C. The small observed differences among the interaction energies, which account for the enthalpic contribution to the free energy of the simulated AQP0-DMPC systems, did

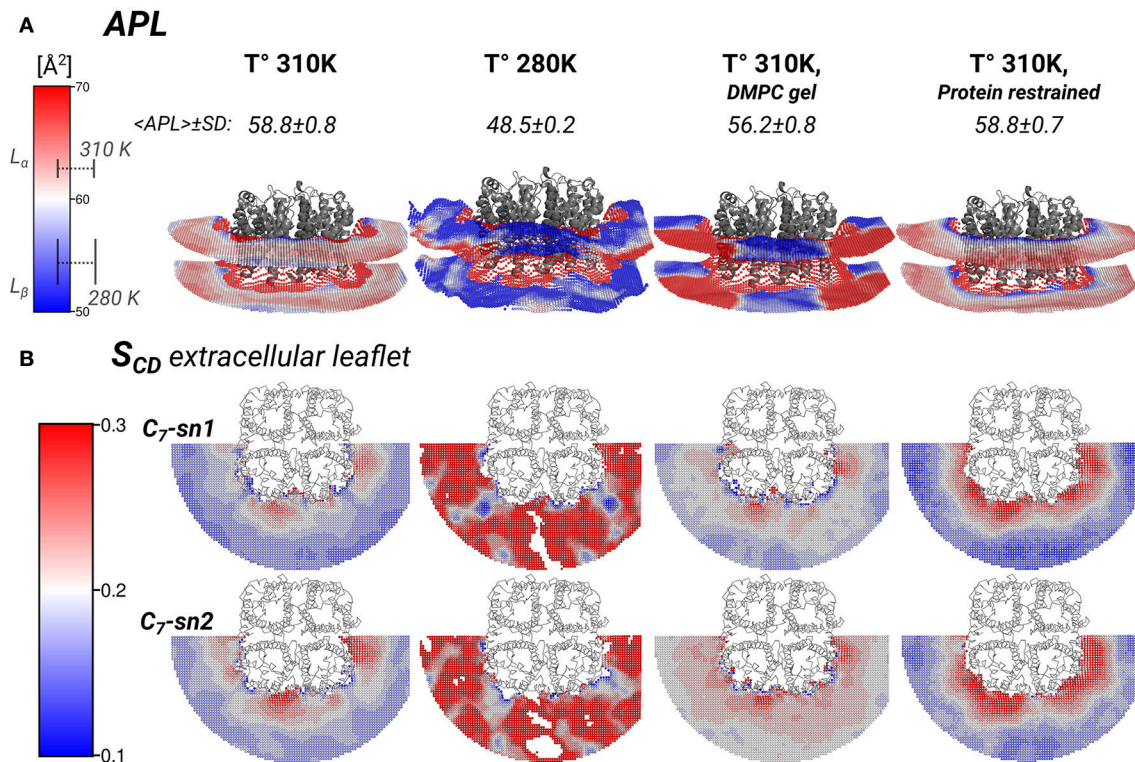


FIGURE 5 | Local area-per-lipid (APL), and S_{CD} order parameters around AQP0 indicate phase prone specific subdomains. Grid elements within 6.5 nm of the tetramer center-of-mass are shown. **(A)** Shows the calculated local and average APL. The color-scale shows the range of APL spanned. The segmented lines on the scale mark the simulated average (\pm SD) values of pure DMPC-water systems. **(B)** Shows the calculated S_{CD} of the carbon-7 (C_7) of both acyl-chains (*sn1* and *sn2*). On the left of the color-scale shows the value range from 0.1 to 0.3. Order parameters lower than 0.1 were omitted in the representations. Extracellular and intracellular S_{CD} of acyl-chain carbons 2, 7, and 13 are shown in Figures S3, S4, respectively.

not explain the increased localization in the annular lipids when restraining the protein. This suggests that the reduction in entropy imposed by restraining the protein crucially contributes to the lipid immobilization.

To address the lipid influence on the protein mobility, we calculated the root-mean-square fluctuations (RMSF) of the protein atoms, and mapped the amino acid contributions to the RMSF on to the protein surface. **Figure 3** showed very similar RMSF profiles for the simulations at 310, 280 K, and for the induced DMPC-gel. These RMSF profiles showed that S2 was the more rigid surface of AQP0, followed by S1. On the contrary, the S1||S2 intra-monomer interface fluctuated more, especially at the extracellular side. These profiles were, as expected, very different to the restrained protein simulation, and suggested that the lipid mobility did not affect the protein flexibility.

Thus, while the restriction of the protein mobility was found to induce lipid ordering, the opposite was not found to be the case: inducing increased lipid ordering did not result in a measurable effect on protein flexibility.

3.3. Lipids Ordering Distribution

The lipid densities showed that the annular lipids localization was most affected by the protein mobility. There were also hexagonal acyl-chain patterns that included the annular lipids on S2, in

all simulated conditions (**Figure 2**). These hexagonal patterns are a local sign of gel-phase ordering introduced on the lipids by an AQP0 tetramer. Gel- or fluid-phase lipid ordering might be observed in its local properties such as thicknesses, area-per-lipid (APL), and carbon-deuterium (S_{CD}) order parameters (Vermeer et al., 2007). These calculated lipid properties were monomer- and time-averaged and, they might suggest the type of hydrophobic mismatch mechanism, the degree of lipid compactness, and the acyl-chain ordering, respectively. The inter-phosphate (P-P) and hydrophobic thicknesses showed that thickening of the annular lipids is the mechanism to compensate for the hydrophobic mismatch in the AQP0-DMPC system at physiological temperature (**Figure 4**). APL and S_{CD} indicated the presence of specific gel- and fluid-phase prone areas around AQP0 (**Figure 5**).

3.3.1. Lipid Thickening Compensate the AQP0-DMPC Hydrophobic Mismatch

Thickening of DMPC around AQP0 compensated the mismatch in the AQP0-DMPC system at physiological temperatures. **Figure 4** shows the inter-phosphate (Thk_{P-P}) and hydrophobic thicknesses (Thk_{hidrop}) calculated around an AQP0 tetramer. Different monomers and the context of surfaces S1 and S2, are shown in **Figure 4A**. The thicknesses (**Figures 4B,C**) were

mapped onto a grid, where the color indicated the thickness value, and the relative *Z*-height in each leaflet, represented the mean position of the atom(s) considered in the calculation (See Methods). For both thicknesses, the color-scale on the left included the average reference values of pure DMPC-water system simulations at 310 K (L_α) and 280 K (L_β).

The free and protein-restrained simulations at 310 K showed clear rims of higher $\text{Thk}_{\text{p-p}}$ and $\text{Thk}_{\text{hidrop}}$ that were in contact with the whole protein surface. These rims increased upon restraining the protein, and they showed slightly lower thicknesses values at the S1||S2 intra-monomer interface. The thickness values of the annular lipids became closer to those of gel-phase DMPC (280 K and induced DMPC-gel simulations), and showed that at physiological temperature DMPC lipids stretched to accommodate to the AQP0 surface. Beyond the annular lipids the $\text{Thk}_{\text{p-p}}$ at 310 K (free and protein-restrained) converged to their bulk values. In the simulations at 280 K and in the induced DMPC-gel, most of the lipids had homogeneous L_β DMPC thicknesses, as expected. This evidence suggests that surface S2 may accommodate longer lipid acyl chains, as indeed observed for *E. coli* polar lipids around AQP0 (Hite et al., 2010). This information indicates that the formation of AQP0 tetrameric arrays is possible under different hydrophobic matching circumstances. Furthermore, it suggests that the lipid accommodation observed here for DMPC may also occur for other more physiologically relevant lipid species beyond *E. coli* polar lipids.

3.3.2. AQP0-DMPC System Shows Specific L_α and L_β Areas

The thickness changes indicated the presence of L_β -like annular lipids, and the lipid densities showed the presence of L_β acyl-chain packing by the S2 AQP0 surface. Those lipid changes might come also with changes in the APL, which reflect the global degree of lipid compactness. In addition, it might be associated with changes in the S_{CD} order parameters that report on the degree of ordering of acyl-chain carbons, which become higher in less mobile acyl-chains (Vermeer et al., 2007; Klauda et al., 2010). Both, APL and S_{CD} might have different values on the extra- or intra-cellular lipid leaflets, and they have characteristic values in L_α and L_β phases. For that purpose, we calculated the local APL (Figure 5A) and the S_{CD} (Figure 5B) around the AQP0 surface. As a reference, the S_{CD} of pure DMPC patches at 280 and 310 K are shown in Figures S3A, S4A.

Local APL and S_{CD} showed very similar phase-prone areas around AQP0. In the case of APL (Figure 5A), we found that the most compact (L_β) lipid surfaces were those close to S2. In the free and restrained protein simulations at 310 K we found areas of low APL (*shades of blue*) near the protein surface. The presence of these areas was an indication of more packed lipids compared with the rest of the patch. These low APL areas coincided with the location of high annular lipid density, as it was observed in the extended low APL rim around the whole AQP0 tetramer in the restrained protein simulation. The average APL of both simulations converged close to their bulk values. As expected from gel-phase lipids, mostly low APL lipids were observed in the 280 K simulation case. Interestingly, the induced DMPC-gel simulation showed two distinct areas: one around the S2||S1

inter-monomer interface that showed low APL, and the S1||S2 intra-monomer surface, which showed higher APL and higher mobility (Figure 3). This APL evidence suggests that the less mobile parts of the protein are able to induce a more compact (gel-like) lipid domain, whereas the more mobile parts, are surrounded by more fluid-like regions. In addition, this evidence indicates that annular lipids are compactly packed around the AQP0 surface.

Similarly to the APL, the distribution of S_{CD} showed two different phase prone areas. In the presence of AQP0, the S_{CD} of the acyl-chains of the extracellular leaflet became more ordered compared to the intracellular one. Extracellular and intracellular S_{CD} plots of carbons 2, 7, and 13 are shown in Figures S3, S4, respectively. As reference Figures S3A, S4A show the S_{CD} profiles calculated on a DMPC-water system simulated at 280 and 310 K. As an example of the lipid ordering, the extracellular S_{CD} of the carbon-7 from both acyl-chains are shown in Figure 5B. It became clear that the S_{CD} were also locally affected by the changes in the protein mobility. In this case also, higher acyl-chain carbon ordering was observed mainly near the S2 surface, while lower order was observed by the S1||S2 intra-monomer surface. Lipids S_{CD} approached to the DMPC bulk values, the further away they were from the AQP0 surface.

In silico mutations of the strongly interacting residues on S2 with DMPC (Aponte-Santamaría et al., 2012) did not substantially modify the lipid positions, and similar packed acyl-chain densities were always observed in the mutant simulations. This evidence suggests that a specific amino acids sequence on the S2 surface is not necessary to promote the gel-like packing of lipids in this region. Instead, we think, that the aquaporin fold, containing six tightly packed transmembrane helices, largely defines the rigid regions that are particularly effective to immobilize lipid molecules. Indeed, different aquaporins (sharing the same protein fold) displayed conserved lipid-protein interaction patterns (Stansfeld et al., 2013). Furthermore, we think the lipid distributions and ordering of a single AQP0-DMPC system are compatible with the observed AQP0 squared arrays separated by an ordered lipid layer.

4. CONCLUSIONS

In this work, we estimated the lipid localization and ordering under different temperatures, phases, and protein mobility. It was revealed that protein mobility largely dominates the annular lipid localization. Surprisingly, the opposite does not hold: lipid immobilization was not found to significantly affect protein mobility. The S2 surface of AQP0 was able to induce lipid localization in and beyond the annular lipid layer, also at 310 K. Local lipid properties indicated that thickening and ordering of DMPC annular lipids is the mechanism by which the AQP0-DMPC system compensates the hydrophobic mismatch at physiological temperatures.

The area-per-lipid and the S_{CD} distributions around AQP0 consistently showed two lipid subdomains, one of gel-like lipid properties close to the S2 surface, which propagated to S1 of the contiguous monomer, and the other of more fluid-like properties at the more mobile S1||S2 interface.

We showed that the AQP0-DMPC system—and probably AQP0 with other similar lipids—displays lipid subdomains of different localization and ordering. These areas might guide the interaction of AQP0 with other membrane components, including the self association of AQP0 copies.

The protein mobility may play an important role, not only for AQP0-DMPC interfaces but also for other systems in which proteins critically modulate the conformational dynamics of their surrounding lipids (Piknová et al., 1993; Niemelä et al., 2010; Stansfeld et al., 2013). Future efforts and progress, from the experimental and computational perspective, may help us to increase our understanding of the nanoscopic details of the lipid-protein interactions.

AUTHOR CONTRIBUTIONS

RB, BD, CA developed the concept of the study. RB prepared the simulations and MD analysis. CA developed the MD density analysis tools and critically revised the manuscript. RB and BD wrote the paper.

REFERENCES

- Abraham, M. J., Murtola, T., Schulz, R., Páll, S., Smith, J. C., Hess, B., et al. (2015). GROMACS: high performance molecular simulations through multi-level parallelism from laptops to supercomputers. *SoftwareX* 1–2, 19–25. doi: 10.1016/j.softx.2015.06.001
- Akabori, K., and Nagle, J. F. (2015). Structure of the DMPC lipid bilayer ripple phase. *Soft Matter* 11, 918–926. doi: 10.1039/c4sm02335h
- Aponte-Santamaría, C., Briones, R., Schenk, A. D., Walz, T., and de Groot, B. L. (2012). Molecular driving forces defining lipid positions around aquaporin-0. *Proc. Natl. Acad. Sci. U.S.A.* 109, 9887–9892. doi: 10.1073/pnas.1121054109
- Baker, M. K., and Abrams, C. F. (2014). Dynamics of lipids, cholesterol, and transmembrane α -helices from microsecond molecular dynamics simulations. *J. Phys. Chem. B* 118, 13590–13600. doi: 10.1021/jp507027t
- Bjelkmar, P., Larsson, P., Cuendet, M. A., Hess, B., and Lindahl, E. (2010). Implementation of the CHARMM force field in GROMACS: analysis of protein stability effects from correction maps, virtual interaction sites, and water models. *J. Chem. Theory Comput.* 6, 459–466. doi: 10.1021/ct900549r
- Boonstra, S., Onck, P. R., and Giessen, E. V. d. (2016). CHARMM TIP3p water model suppresses peptide folding by solvating the unfolded state. *J. Phys. Chem. B* 120, 3692–3698. doi: 10.1021/acs.jpcc.6b01316
- Borchman, D., and Yappert, M. C. (2010). Lipids and the ocular lens. *J. Lipid. Res.* 51, 2473–2488. doi: 10.1194/jlr.R004119
- Bussi, G., Donadio, D., and Parrinello, M. (2007). Canonical sampling through velocity rescaling. *J. Chem. Phys.* 126:014101. doi: 10.1063/1.2408420
- Chepelinsky, A. B. (2009). “Structural function of MIP/Aquaporin-0 in the eye lens; genetic defects lead to congenital inherited cataracts,” in *Aquaporins*, ed E. Beitz (Berlin-Heidelberg: Springer), 265–297.
- Colom, A., Casuso, I., Boudier, T., and Scheuring, S. (2012). High-speed atomic force microscopy: cooperative adhesion and dynamic equilibrium of junctional microdomain membrane proteins. *J. Mol. Biol.* 423, 249–256. doi: 10.1016/j.jmb.2012.07.004
- Colom, A., Casuso, I., Rico, F., and Scheuring, S. (2013). A hybrid high-speed atomic force-optical microscope for visualizing single membrane proteins on eukaryotic cells. *Nat. Commun.* 4:2155. doi: 10.1038/ncomms3155
- Costello, M. J., McIntosh, T. J., and Robertson, J. D. (1989). Distribution of gap junctions and square array junctions in the mammalian lens. *Invest. Ophthalmol. Vis. Sci.* 30, 975–989.
- de Planque, M. R. R., and Killian, J. A. (2003). Protein-lipid interactions studied with designed transmembrane peptides: role of hydrophobic

FUNDING

The Deutsche Forschungsgesellschaft (DFG) Sonderforschungsbereich (SFB) 803: Project A03 to RB and BD. This work was supported by grants from the Max Planck Society (CA and BD), the German Research Foundation to the Research Group FOR1543 (CA), and the BIOMS postdoctoral program of the Heidelberg University (CA).

ACKNOWLEDGMENTS

We acknowledge Andreas Schenk and Tom Walz for their useful discussions.

SUPPLEMENTARY MATERIAL

The Supplementary Material for this article can be found online at: <http://journal.frontiersin.org/article/10.3389/fphys.2017.00124/full#supplementary-material>

- matching and interfacial anchoring (review). *Mol. Membr. Biol.* 20, 271–284. doi: 10.1080/09687680310001605352
- Dumas, F., Sperotto, M. M., Lebrun, M.-C., Tocanne, J.-F., and Mouritsen, O. G. (1997). Molecular sorting of lipids by bacteriorhodopsin in dilauroylphosphatidylcholine/distearoylphosphatidylcholine lipid bilayers. *Biophys. J.* 73:1940.
- Essmann, U., Perera, L., Berkowitz, M. L., Darden, T., Lee, H., and Pedersen, L. G. (1995). A smooth particle mesh Ewald method. *J. Chem. Phys.* 103:8577. doi: 10.1063/1.470117
- Fowler, P. W., Hélie, J., Duncan, A., Chavent, M., Koldsø, H., and Sansom, M. S. P. (2016). Membrane stiffness is modified by integral membrane proteins. *Soft Matter* 12, 7792–7803. doi: 10.1039/C6SM01186A
- Gapsys, V., de Groot, B. L., and Briones, R. (2013). Computational analysis of local membrane properties. *J. Comput. Aided Mol. Des.* 27, 845–858. doi: 10.1007/s10822-013-9684-0
- Gonen, T., Cheng, Y., Sliz, P., Hiroaki, Y., Fujiyoshi, Y., Harrison, S. C., et al. (2005). Lipid-protein interactions in double-layered two-dimensional AQP0 crystals. *Nature* 438, 633–638. doi: 10.1038/nature04321
- Gonen, T., Sliz, P., Kistler, J., Cheng, Y., and Walz, T. (2004). Aquaporin-0 membrane junctions reveal the structure of a closed water pore. *Nature* 429, 193–197. doi: 10.1038/nature02503
- Gupta, K., Donlan, J. A. C., Hopper, J. T. S., Uzdaviny, P., Landreh, M., Struwe, W. B., et al. (2017). The role of interfacial lipids in stabilizing membrane protein oligomers. *Nature* 541, 421–424. doi: 10.1038/nature20820.
- Hirai, T., Mitsuoka, K., Kidera, A., and Fujiyoshi, Y. (2007). Simulation of charge effects on density maps obtained by high-resolution electron crystallography. *J. Electron Microsc.* 56, 131–140. doi: 10.1093/jmicro/dfm019
- Hite, R. K., Li, Z., and Walz, T. (2010). Principles of membrane protein interactions with annular lipids deduced from aquaporin-0 2d crystals. *EMBO J.* 29, 1652–1658. doi: 10.1038/emboj.2010.68
- Jorgensen, W. L., Chandrasekhar, J., Madura, J. D., Impey, R. W., and Klein, M. L. (1983). Comparison of simple potential functions for simulating liquid water. *J. Chem. Phys.* 79, 926. doi: 10.1063/1.445869
- Kandasamy, S. K., and Larson, R. G. (2006). Molecular dynamics simulations of model trans-membrane peptides in lipid bilayers: a systematic investigation of hydrophobic mismatch. *Biophys. J.* 90, 2326–2343. doi: 10.1529/biophysj.105.073395
- Killian, J. A. (1998). Hydrophobic mismatch between proteins and lipids in membranes. *Biochim. Biophys. Acta* 1376, 401–415.

- Kim, T., and Im, W. (2010). Revisiting hydrophobic mismatch with free energy simulation studies of transmembrane helix tilt and rotation. *Biophys. J.* 99, 175–183. doi: 10.1016/j.bpj.2010.04.015
- Kim, T., Lee, K., Morris, P., Pastor, R., Andersen, O., and Im, W. (2012). Influence of hydrophobic mismatch on structures and dynamics of Gramicidin A and lipid bilayers. *Biophys. J.* 102, 1551–1560. doi: 10.1016/j.bpj.2012.03.014
- Klauda, J. B., Venable, R. M., Freites, J. A., O'Connor, J. W., Tobias, D. J., Mondragon-Ramirez, C., et al. (2010). Update of the CHARMM all-atom additive force field for lipids: validation on six lipid types. *J. Phys. Chem. B* 114, 7830–7843. doi: 10.1021/jp101759q
- Laganowsky, A., Reading, E., Allison, T. M., Ulmschneider, M. B., Degiacomi, M. T., Baldwin, A. J., et al. (2014). Membrane proteins bind lipids selectively to modulate their structure and function. *Nature* 510, 172–175. doi: 10.1038/nature13419
- Landreh, M., Marty, M. T., Gault, J., and Robinson, C. V. (2016). A sliding selectivity scale for lipid binding to membrane proteins. *Curr. Opin. Struct. Biol.* 39, 54–60. doi: 10.1016/j.sbi.2016.04.005
- Lee, A. (2003). Lipid–protein interactions in biological membranes: a structural perspective. *Biochim. Biophys. Acta* 1612, 1–40. doi: 10.1016/S0005-2736(03)00056-7
- Lee, A. G. (2011). Biological membranes: the importance of molecular detail. *Trends Biochem. Sci.* 36, 493–500. doi: 10.1016/j.tibs.2011.06.007
- MacKerell, A. D., Bashford, D., Bellott, M., Dunbrack, R. L., Evanseck, J. D., Field, M. J., et al. (1998). All-atom empirical potential for molecular modeling and dynamics studies of proteins. *J. Phys. Chem. B* 102, 3586–3616. doi: 10.1021/jp973084f
- Marsh, D. (2008). Protein modulation of lipids, and vice-versa, in membranes. *Biochim. Biophys. Acta* 1778, 1545–1575. doi: 10.1016/j.bbamem.2008.01.015
- Monticelli, L., Tieleman, D. P., and Fuchs, P. F. (2010). Interpretation of ^2H -NMR experiments on the orientation of the transmembrane helix WALP23 by computer simulations. *Biophys. J.* 99, 1455–1464. doi: 10.1016/j.bpj.2010.05.039
- Niemelä, P. S., Miettinen, M. S., Monticelli, L., Hammaren, H., Bjelkmar, P., Murtola, T., et al. (2010). Membrane proteins diffuse as dynamic complexes with lipids. *J. Am. Chem. Soc.* 132, 7574–7575. doi: 10.1021/ja101481b
- Nosé, S., and Klein, M. (1983). Constant pressure molecular dynamics for molecular systems. *Mol. Phys.* 50, 1055–1076. doi: 10.1080/00268978300102851
- O'Connor, J. W., and Klauda, J. B. (2011). Lipid membranes with a majority of cholesterol: applications to the ocular lens and aquaporin 0. *J. Phys. Chem. B* 115, 6455–6464. doi: 10.1021/jz200167q
- Pastor, R. W., and MacKerell, A. D. (2011). Development of the CHARMM force field for lipids. *J. Phys. Chem. Lett.* 2, 1526–1532. doi: 10.1021/jz200167q
- Piknová, B., Pérochon, E., and Tocanne, J.-F. (1993). Hydrophobic mismatch and long-range protein/lipid interactions in bacteriorhodopsin/phosphatidylcholine vesicles. *Eur. J. Biochem.* 218, 385–396.
- Schrödinger, L. L. C. (2015). *The PyMOL Molecular Graphics System, Version 1.8*. New York, NY.
- Smith, G. S., Sirota, E. B., Safinya, C. R., Plano, R. J., and Clark, N. A. (1990). X-ray structural studies of freely suspended ordered hydrated DMPC multimembrane films. *J. Chem. Phys.* 92:4519.
- Stansfeld, P., Jefferys, E., and Sansom, M. (2013). Multiscale simulations reveal conserved patterns of lipid interactions with aquaporins. *Structure* 21, 810–819. doi: 10.1016/j.str.2013.03.005
- Swope, W. C. (1982). A computer simulation method for the calculation of equilibrium constants for the formation of physical clusters of molecules: application to small water clusters. *J. Chem. Phys.* 76:637. doi: 10.1063/1.442716
- Vermeer, L. S., de Groot, B. L., Réat, V., Milon, A., and Czaplicki, J. (2007). Acyl chain order parameter profiles in phospholipid bilayers: computation from molecular dynamics simulations and comparison with ^2H -NMR experiments. *Eur. Biophys. J.* 36, 919–931. doi: 10.1007/s00249-007-0192-9
- Yin, F., and Kindt, J. (2012). Hydrophobic mismatch and lipid sorting near OmpA in mixed bilayers: atomistic and coarse-grained simulations. *Biophys. J.* 102, 2279–2287. doi: 10.1016/j.bpj.2012.04.005

Conflict of Interest Statement: The authors declare that the research was conducted in the absence of any commercial or financial relationships that could be construed as a potential conflict of interest.

Copyright © 2017 Briones, Aponte-Santamaría and de Groot. This is an open-access article distributed under the terms of the Creative Commons Attribution License (CC BY). The use, distribution or reproduction in other forums is permitted, provided the original author(s) or licensor are credited and that the original publication in this journal is cited, in accordance with accepted academic practice. No use, distribution or reproduction is permitted which does not comply with these terms.